Image analysis for classification of damaged and undamaged areas on composite structures

Shrestha, Pratik; Groves, Roger M.

DOI
10.1117/12.2513430

Publication date
2019

Document Version
Final published version

Published in
Nondestructive Characterization and Monitoring of Advanced Materials, Aerospace, Civil Infrastructure, and Transportation XIII

Image analysis for classification of damaged and undamaged areas on composite structures

Pratik Shrestha, Roger M. Groves

Pratik Shrestha, Roger M. Groves, "Image analysis for classification of damaged and undamaged areas on composite structures ," Proc. SPIE 10971, Nondestructive Characterization and Monitoring of Advanced Materials, Aerospace, Civil Infrastructure, and Transportation XIII, 109711C (1 April 2019); doi: 10.1117/12.2513430

SPIE.

Event: SPIE Smart Structures + Nondestructive Evaluation, 2019, Denver, Colorado, United States

Image analysis for classification of damaged and undamaged areas on composite structures

Pratik Shrestha*[a], Roger M. Groves[a]
[a]Aerospace Non-Destructive Testing Laboratory, Faculty of Aerospace Engineering, TU Delft, Kluyverweg 1, 2629 HS Delft, The Netherlands

ABSTRACT

Composite materials are susceptible to barely visible impact damages (BVID) due to low-velocity impact. Therefore, an automated damage detection and quantification technique is highly desirable for quick inspection of large number of composite structures. Among various different non-destructive techniques (NDTs), active thermography NDT can be used for detecting damage on aircraft structures, using an infrared camera to capture the temperature distribution on the structure after it is exposed to heat using a flash lamp. In this paper, an image analysis algorithm that analyzes the infrared image, acquired using NDTherm NT, by determining the changes in the colormap values to automate the detection and quantification of the damage size was proposed. An area of the second derivative pre-processed grayscale image acquired using NDTherm NT is scanned in the x-direction and y-direction, and for each scan region the histogram of colormap values is extracted and stored. Irregularities in the structure result in non-uniform temperature distributions, which cause the infrared image to have a wide-range of grayscale colormap values in the damaged area. Therefore, the damage region is identified by monitoring the changes in the number of detected grayscale colormap values. The proposed image analysis technique was implemented for automated damage detection on Boeing 787 skin's curved CFRP panel, with dimensions of 1.3 × 1.3 m. The proposed method detected the damage and determined the maximum damage length in the x-direction and y-direction to be 70.1 mm and 57.8 mm, respectively. Moreover, the proposed technique is suitable for feature identification applications.

Keywords: BVID, composite material, damage monitoring, image analysis, NDT, thermography.

1. INTRODUCTION

The number of aircraft with over 100 seats is expected to double and reach over 47000 in the next 20 years[1]. Additionally, composite materials are being used significantly for manufacturing aircraft components; 50% of the airframe in the Boeing 787[2] and 53% of the airframe in the Airbus A350XWB[3] are made using composite materials. These materials are susceptible to barely visible impact damages upon impact due to impact events such as runway debris, tool drop and bird strike[4]. In the year 2007, fight delays cost airlines an estimated $32.9 billion[5]. Moreover, this cost can be expected to rise significantly as well in the next 20 years due to grounded aircraft. Therefore, significant growth in the demand for non-destructive techniques (NDT) such as radiography[6], phased arrays ultrasonic testing[7], thermography inspection[8], etc., can be expected for inspecting this large number of aircraft efficiently and accurately.

Most of the inspections are done manually, which is labor intensive, inspection reliability can be low and inspection of difficult to access region can also be risky to the inspection personnel. Therefore, automated robotic inspection systems for inspection of aircraft are needed which are capable of detecting damages on the aircraft structure with minimal human supervision. Such a system can help to improve inspection reliability, perform a large number of inspections in a short time, reduce the duration the aircraft remains grounded and reduce operational costs. There are various damage types for NDT to detect in aircraft structures such as corrosion inspection, crack detection, fatigue damage detection, disbond, moisture detection, material degradation inspection and repair inspection. The damage analysis can be performed by processing and analyzing the signals acquired from the NDT. Moreover, the measured data can be processed to extract the suitable features for supervised or unsupervised machine learning algorithms to recognize patterns to detect, locate and quantify the damage[9]. Classification of damaged and undamaged data can be performed using novelty detection methods based on clustering techniques such as fuzzy clustering[10] and density peaks-based fast

*P.Shrestha@tudelft.nl; phone +31 15 27 86522; web https://www.tudelft.nl/en/ae/

Nondestructive Characterization and Monitoring of Advanced Materials, Aerospace, Civil Infrastructure, and Transportation XIII, edited by A. L. Gyekenyesi, T.-Y. Yu, H. F. Wu, P. J. Shull, Proc. of SPIE Vol. 10971
109711C · © 2019 SPIE · CCC code: 0277-786X/19/$18 · doi: 10.1117/12.2513430

clustering[11]. The feature extraction and cluster techniques can reduce the complexity in processing big data acquired when monitoring large scale structures. Reyno et al. used a 3D laser scanner to determine the damage dimensions on honeycomb sandwich panels by comparing the 3D scan point cloud with surface fit data of the undamaged surface[12]. Xu et al. used eddy current pulsed thermography and infrared image sequences processing using principal component analysis to detect cracks on corroded metal surface[13]. Liang et al. combined principal component analysis and wavelet transform to process thermal images for improving the detectability of internal damages on composite structures[14]. Cha et al. proposed a vision based damage detection technique using deep-learning convolutional neural networks for detecting cracks[15].

In this paper, image analysis of an infrared image acquired using thermographic inspection was performed to assess the colormap data for the purpose of automated damage detection, localization and quantification on composite structure. The paper is organized as follows: i) in Section 2, the experimental setup is presented, ii) in Section 3, the image analysis algorithm is described, ii) in Section 4, the results and discussions of the training dataset and test dataset are presented, and iii) finally the conclusions and future works are presented in Section 5.

2. EXPERIMENTAL SETUP

In this section, the experimental setup for acquiring infrared images of a damaged composite panel for training and testing the developed image analysis algorithm is presented. A portable thermographic inspection device, NDTherm NT, was used to detect the BVID on a damaged CFRP panel of Boeing 787's fuselage skin with dimensions of 1.3 × 1.3 × 0.0038 m and a radius of 2 m, by TiaT Europe at TU Delft. The experimental setup is shown in Figure 1. The NDTherm NT consists of a flash lamp for heating the test structure's surface and an infrared camera for acquiring the temperature distribution which is stored as an image file. The image data acquired by the NDTherm NT is used as the input data for the image analysis algorithm developed to detect, localize and quantify the internal damage on the CFRP panel. The overview of the image analysis algorithm is presented in the following section.

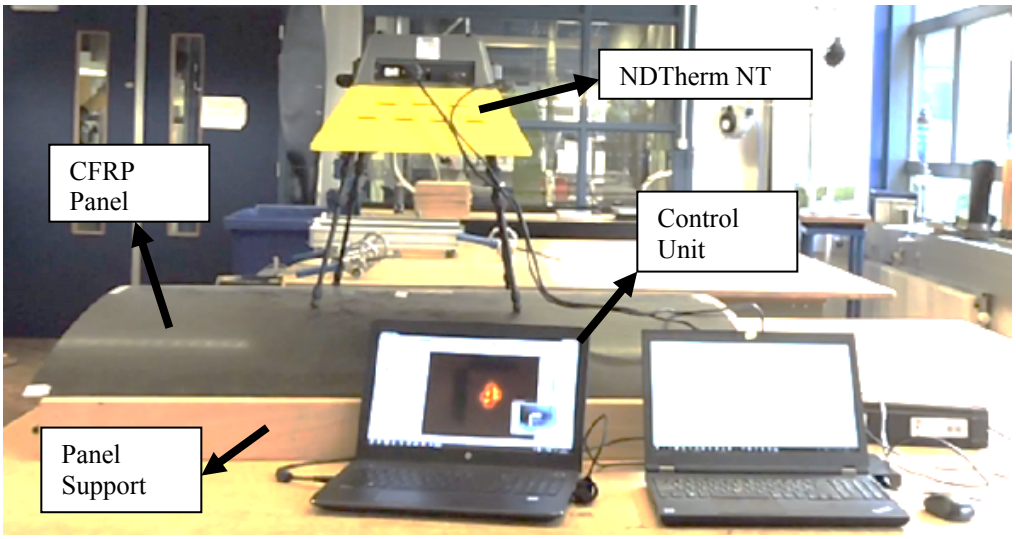

Figure 1. Experimental setup for thermographic inspection of the CFRP panel.

3. IMAGE ANALYSIS ALGORITHM

In this section, an image analysis algorithm that extracts a number of colormap value features from a grayscale image acquired using a portable thermographic inspection for automated damage assessment is presented. In the image analysis algorithm, three key tasks are performed to determine the location and size of the damage on the CFRP panel: a) data pre-processing, b) possible damage location identification and c) classification of the damaged and undamaged region. The overview of the algorithm is presented in Figure 2.

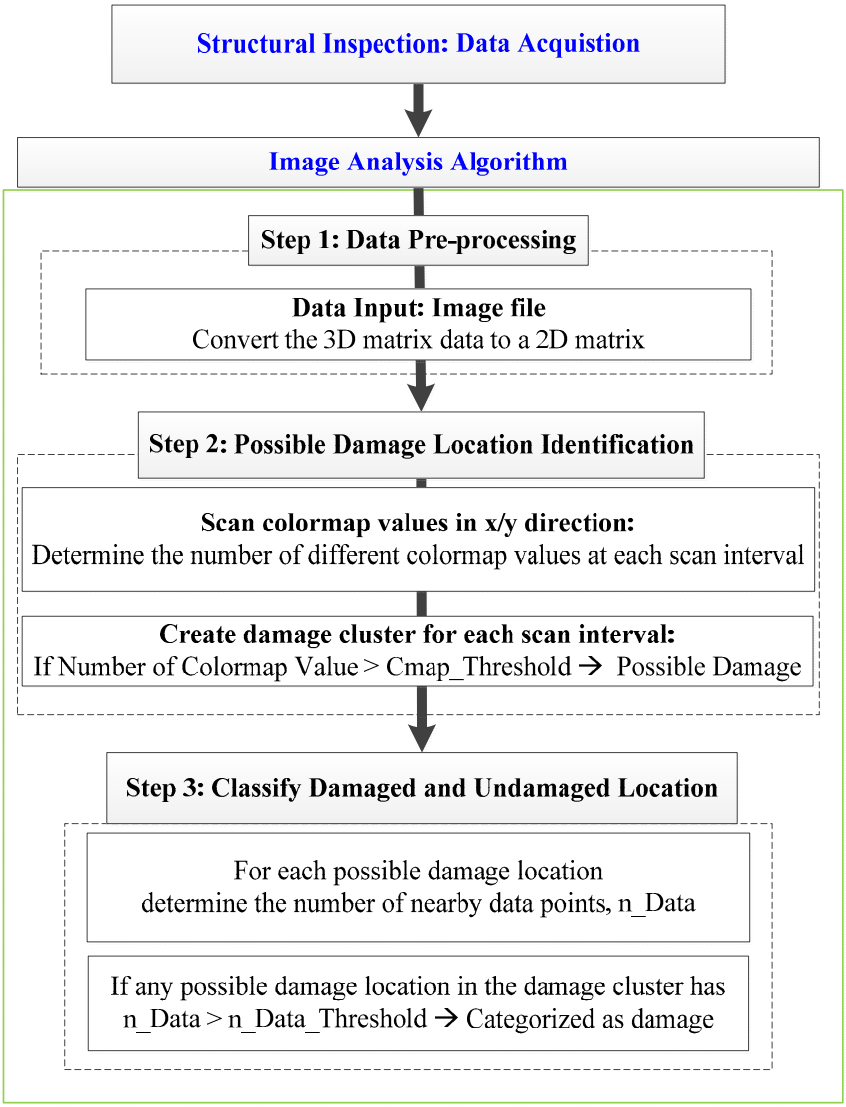

Figure 2. Overview of image processing algorithm for damage analysis.

An image data consists of an $m \times n$ number of pixels, and each pixel corresponds to a particular location and intensity. The intensity of the pixel is stored as a number in matrix. One of the commonly used color representation models used in computers is the RGB color model, which is an additive color model[16]. In the RGB color model, the colors are reproduced by combining the red (R), green (G) and blue (B) light components. The colors in images are represented using a colormap, which consists of the three color components in a 3D matrix, $m \times n \times 3$ matrix. In an 8-bit image RGB color model, the color is defined using variables of class uint8 with R, G, and B values, which can vary from a minimum value of 0 to maximum value of 255. The grayscale images have pixel values of R=G=B. The minimum R=G=B=0 represents black color and maximum R=G=B=255 represents white color.

The first step of the image analysis algorithm involves data pre-processing of the $m \times n \times 3$ matrix. In this step, a new matrix is created that consists of the property of each pixel such as RBG colormap values and the coordinates values. The 2D matrix containing the colormap data, $P[R_{x,y}, G_{x,y}, B_{x,y}]$, is constructed by transforming the image components stored in 3D matrix; where $x = 1$ to m, and $y = 1$ to n. Subsequently, a size marker with a known dimension was used to calculate the size of the test panel in SI units and a matrix containing the x-coordinates and y-coordinates of each pixel is created. Since the image used is 2D the z-component data of each pixel is not known, therefore, in the present algorithm, the z-coordinate of each point is assigned with an equal value. Finally, each surface point, $[S_x, S_y]$, is assigned with the corresponding colormap value, $P[R_{x,y}, G_{x,y}, B_{x,y}]$. The data pre-processing process is illustrated in Figure 3.

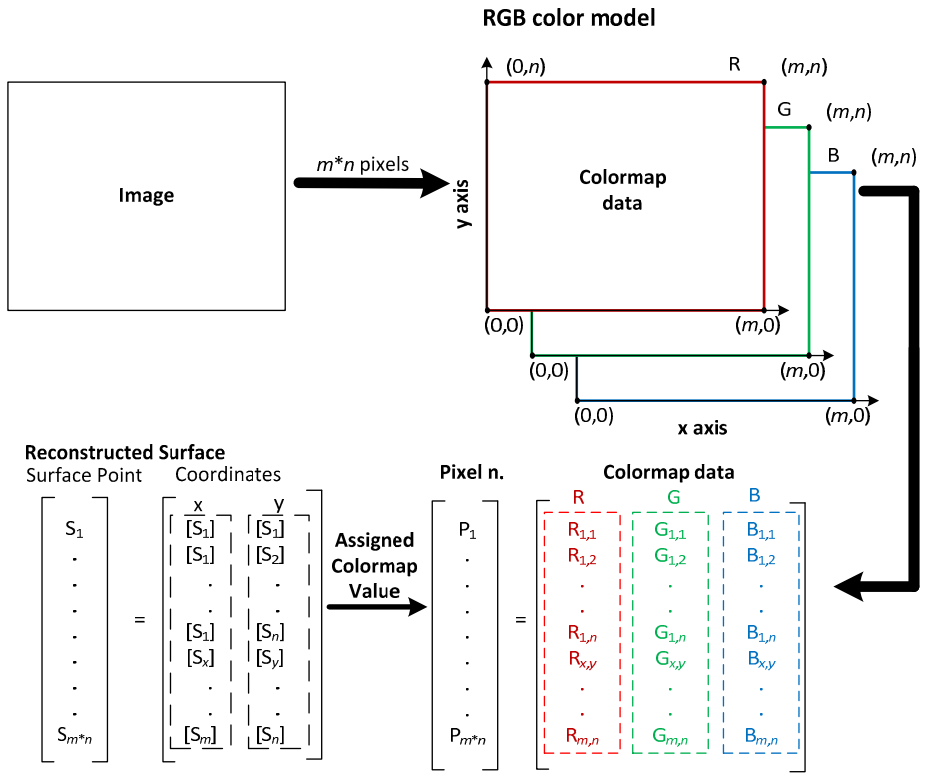

Figure 3. Illustration of data pre-processing procedure.

In step 2, the possible damage location identification is done by analyzing the pre-processed data. First, the feature selection and extraction is performed to reduce the volume of data required for damage analysis and to simplify the damage analysis process. In the case of the thermography inspection, the damage is detected by observing the difference in the temperature distribution. The presence of damage results in an uneven distribution of temperature detected by the infrared camera. Therefore, in the scan region with the damage the number of different colormap values detected can be expected to be higher than in the undamaged region. So, the variation in the detected number of colormap values was selected as the feature for damage detection. Clusters with the colormap values feature were created by scanning the image data in the x-direction for $y = 1$ to n and in the y-direction for $x = 1$ to m. Subsequently, comparison of the number of colormap values feature detected at each cluster is analyzed for determining the possible damage location is done. If the detected number of colormap values is greater than the Cmap_Threshold value then it is categorized as a possible damage location. The Cmap_Threshold value was determined through a preliminary parametric study by observing the damaged area detected for a training dataset of various threshold values.

Finally in Step 3, the classification of the damaged and undamaged area is done. In this step, a second cluster matrix, consisting of a cluster of possible damage locations for each scan direction is created by determining the number of nearby data points that are above the n_Data_Threshold, which is set to 10. If a possible damage location has more than 10 other nearby possible damage detected location then it is classified as damaged, otherwise, it is classified as undamaged location.

4. RESULTS AND DISCUSSIONS

In this section, the results of the image analysis algorithm developed for automated damage monitoring are presented. The damaged CFRP panel was inspected using NDTherm NT and the grayscale infrared images were obtained. The infrared images of two datasets with the impact damage are shown in Figure 4. These datasets were used to train and test the damage localization and quantification algorithm.

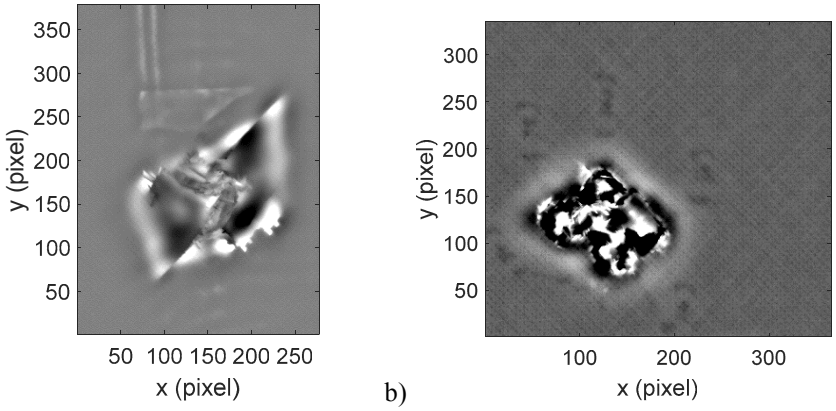

Figure 4. a) Case A: training dataset and b) Case B: test dataset.

First, the Case A image data, with 277 × 378 pixels, was used for training the algorithm to identify the presence of damage visible on the mid-region of the image. The image data was first pre-processed to convert the 277 × 378 × 3 3D matrix to a 104706 × 3 2D matrix. A size marker was used to determine the size of the image from pixel to SI unit. The size of Case A was determined to be 103.4 mm × 141.0 mm. Subsequently, the pre-processed data was analyzed to determine the number of different colormap values in the x-direction and y-direction, as shown in Figure 5. This feature extraction process significantly reduced the volume of data required for damage analysis. In total, 664 clusters were created and from each cluster, a single feature, the number of colormap values present in the cluster, were obtained for the damage analysis in the next step of the algorithm.

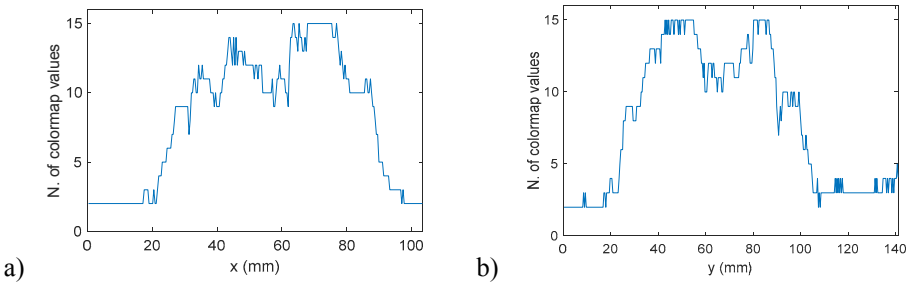

Figure 5. N. of colormap value feature extraction in a) x-direction scan and b) y-direction scan.

In Figure 5, it can be seen that the number of colormap values detected in the 664 clusters ranges from 2 to 15. The lowest number of colormap values corresponds to the undamaged area and the increase in the number of colormap values is a result of the presence of damage observed in the image shown in Figure 4 (a). In order to determine a suitable Cmap_Threshold for the algorithm, a parametric study was performed by calculating the detected damage area for Cmap_Threshold values from 1 to 8.

The area detected as damage for Cmap_Threshold value of 1 to 8 is presented in Figure 6. Since the minimum number of detected colormap value is 2, the lowest threshold value of 1 resulted in the entire panel being classified as damaged. By increasing the threshold value it can be seen that the size of the detected damage area is reduced. Cmap_Threshold of 2 and 3 resulted in the damage length in x-direction and y-direction to be within the range of 70.0 mm and 124.0 mm, respectively. When the Cmap_Threshold of 2 or 3 was selected, the damage length in the y-direction is found to be longer in the y-direction due to detection of the two vertical lines located on the upper left quadrant of the image. The vertical lines correspond to visible surface features that are present on the structure. Whereas, with Cmap_Threshold between 4 and 8 the damage region was correctly identified. The damage area was determined to be 67.9 mm × 80.6 mm with Cmap_Threshold = 4, and increasing the threshold value resulted in decrease in the size of the detected damage area. Using Cmap_Threshold = 8, the damaged area was determined to be 61.2 mm × 73.1 mm. From the Cmap_Threshold parametric study, Cmap_Threshold value higher than 2 was found to be suitable for correct identification of the damage region for Case A dataset. Proper Cmap_Threshold selection is important for accurate damage size detection; if it is too small then it can result in overestimation of the damage size and if it is too high then it

can lead to underestimation of the damage size. Based on the results obtained from training dataset, the Cmap_Threshold was set to 5.

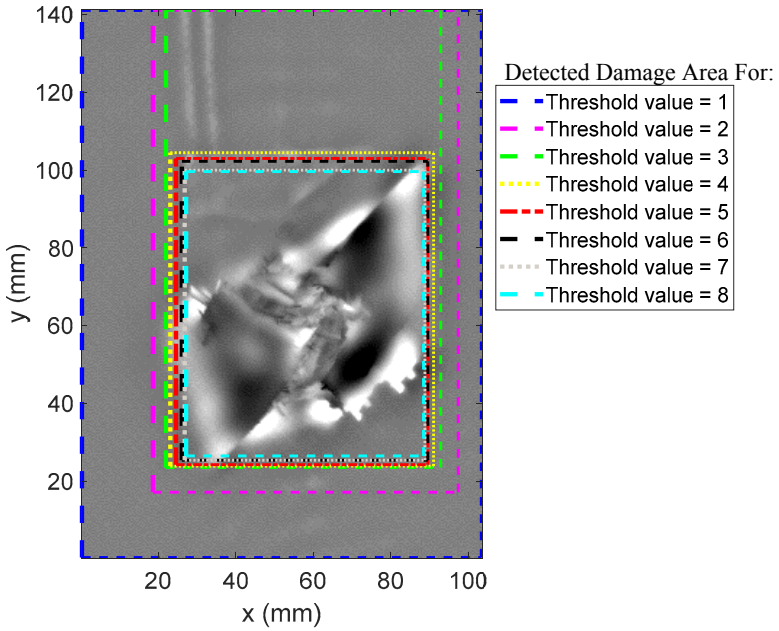

Figure 6. Case A: Damage area detection for Cmap_Threshold value of 1 to 8.

The image analysis algorithm trained using Case A dataset was used to detect the damaged area for Case B dataset, shown in Figure 4 (b). Case B dataset has 365 × 335 pixels and dimensions of 136.2 mm × 125.0 mm. The pre-processing of Case B dataset consisting of 365 × 335 × 3 3D matrix resulted in a 122275 × 3 2D matrix. Subsequently, the feature extraction process output a total of 691 clusters, 27 clusters more than that of Case A, that consists of colormap data for each scan interval. The detected damage location and size result for Case B is shown in Figure 7. In the infrared image, the damage can be observed on the lower left quadrant. Using the image analysis algorithm, the damage location was also determined to be located in the lower left quadrant of the image. The damage size was determined to be 70.1 mm long in the x-direction and 57.8 mm long in the y-direction.

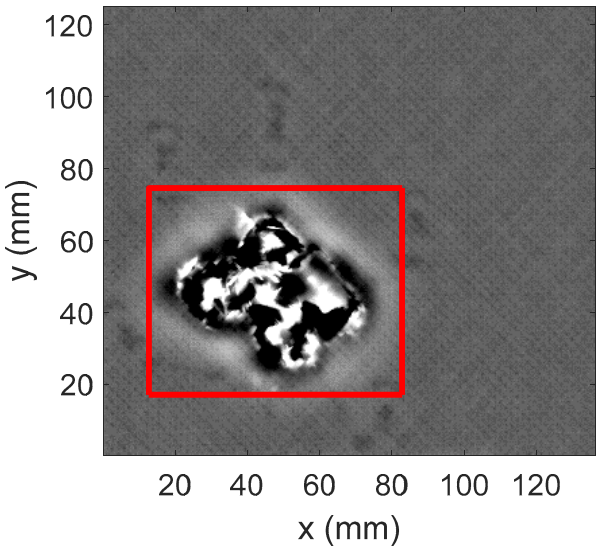

Figure 7. Case B: Damage area detection for Cmap_Threshold value of 5.

In this study, image analysis of two datasets from a damaged CFRP panel was performed. In comparison to the visual damage area identification, the proposed image analysis technique detected damage size results are found to be similar. Therefore the proposed number of colormap value feature is determined to be feasible for detecting the damage and to determine its size. However, one of the limitations of the presented algorithm is that a fixed threshold was used for automated damage detection. Furthermore, the algorithm only determines the size of the damage in the vertical and horizontal direction of the image. Therefore, the algorithm needs to be further developed to detect damages on an image with varying background noise and to detect the orientation of the damage.

5. CONCLUSIONS AND FUTURE WORKS

In this paper, an image analysis algorithm that analyzes the colormap feature to automate the detection, localization and quantification of damage on a composite structure was presented. The developed algorithm was trained and tested using grayscale images acquired using thermography. The results of the image analysis algorithm were found to be sensitive to changes in the Cmap_Threshold value. Lower thresholds can be used to detect small outliers in the dataset, while higher threshold values can be used to tune the algorithm to detect larger deviations that exist in the dataset. The proposed image analysis method was capable of localizing and quantifying the damage on the CFRP panel. Further work is needed to improve and assess the performance of the proposed algorithm for damage monitoring applications. The proposed data analysis method can be incorporated in an automated NDT system that can be used to inspect large scale structures such as an aircraft using robots for damage detection and analysis. Moreover, the proposed image analysis technique can be used for various other applications such as damage detection in bridges, wind turbine and also in other fields where image feature identification is required.

ACKNOWLEDGEMENTS

This research was supported by the Defense Technology Project ‘Development of Technology for Depot Repairs of Composite Structures’, SID:11691, supported by the Royal Netherlands Air Force. The authors would like to thank Mr. Pieter Troost, TiaT Europe BV, for his assistance with the thermographic inspection.

REFERENCES

[1] Airbus., “Global Market Forecast 2018-2037” (2018).
[2] Hale, J., “Boeing 787 from the ground up,” Aero QTR_04, 17–23 (2006).
[3] “FAST (Flight Airworthiness Support Technology)—Special Edition A350XWB.”, Airbus Tech. Mag. (2013).
[4] Shyr, T.-W. and Pan, Y.-H., “Impact resistance and damage characteristics of composite laminates,” Compos. Struct. 62(2), 193–203 (2003).
[5] Ball, M., Barnhart, C., Dresner, M., Hansen, M., Neels, K., Odoni, A., Peterson, E., Sherry, L., Antonio, T. and Zou, B., “Total delay impact study : a comprehensive assessment of the costs and impacts of flight delay in the United States,” Washington, D.C (2010).
[6] Wang, X., Wong, B. S., Tan, C. and Tui, C. G., “Automated Crack Detection for Digital Radiography Aircraft Wing Inspection,” Res. Nondestruct. Eval. 22(2), 105–127 (2011).
[7] McNab, A. and Campbell, M. J., “Ultrasonic phased arrays for nondestructive testing,” NDT Int. 20(6), 333–337 (1987).
[8] Chrysafi, A. P., Athanasopoulos, N. and Siakavellas, N. J., “Damage detection on composite materials with active thermography and digital image processing,” Int. J. Therm. Sci. 116, 242–253 (2017).
[9] Bishop, C. M., [Pattern Recognition and Machine Learning], Springer New York (2006).
[10] Silva, S. D., Júnior, M. D., Junior, V. L. and Brennan, M. J., “Structural damage detection by fuzzy clustering,” Mech. Syst. Signal Process. 22(7), 1636–1649 (2008).
[11] Cha, Y.-J. and Wang, Z., “Unsupervised novelty detection–based structural damage localization using a density peaks-based fast clustering algorithm,” Struct. Heal. Monit. 17(2), 313–324 (2018).
[12] Reyno, T., Marsden, C. and Wowk, D., “Surface damage evaluation of honeycomb sandwich aircraft panels using 3D scanning technology,” NDT E Int. 97, 11–19 (2018).

[13] Xu, C., Zhou, N., Xie, J., Gong, X., Chen, G. and Song, G., "Investigation on eddy current pulsed thermography to detect hidden cracks on corroded metal surface," NDT E Int. 84, 27–35 (2016).
[14] Liang, T., Ren, W., Tian, G. Y., Elradi, M. and Gao, Y., "Low energy impact damage detection in CFRP using eddy current pulsed thermography," Compos. Struct. 143, 352–361 (2016).
[15] Cha, Y.-J., Choi, W. and Büyüköztürk, O., "Deep Learning-Based Crack Damage Detection Using Convolutional Neural Networks," Comput. Civ. Infrastruct. Eng. 32(5), 361–378 (2017).
[16] Rhyne, T.-M., [Applying color theory to digital media and visualization], CRC Press (2016).